한국소음진동공학회 1995년도 추계학술대회논문집 pp. 154-159

확장된 영향계수법을 이용한 능동자기베어링의 운전상황에서 측정체 진원도 오차 규명

0김 철 순,* 이 종 원**

(In-situ Runout Identification in Active Magnetic Bearing System by Extended Influence Coefficient Method)

(Cheol-Soon Kim, Chong-Won Lee)

Abstract

In this study, an efficient, yet easy to use, in-situ runout identification scheme by using extended influence coefficient method is presented for active magnetic bearing(AMB) systems. It is shown experimentally that the proposed scheme successfully identifies and eliminates the troublesome runout of the well balanced AMB system in the laboratory so that a high precision spindle system can be achieved, while it is in operation.

Introduction

Active magnetic bearing(AMB) systems have drawn much attention among many researchers in rotor dynamics field, since they have been widely used in industry due to the advantages such as: free of contact and lubrication, high peripheral speed and precision operation, and adjustability of the bearing stiffness and damping up to their physical limits[1]. AMB systems always require the feedback control of magnetic force using measured displacement of rotor for stable levitation. And the positioning accuracy of an AMB system essentially depends on the quality of measured signals, which is strongly dependent upon the resolution of the sensors in use and the presence of sensing target runout. The displacement of a rotor may be measured by using non-contacting proximity measuring devices such as optical devices, eddy-current probes, capacitive probes, or inductive types. And the measured signals are affected by mechanical or electrical runout of sensing target. The mechanical runout is caused by nonconcentric rotors or surface irregularities while the electrical runout is caused by residual magnetics, metallurgical microscopic segregation or localized stress concentration[2].

The runout of sensing target in an AMB system acts as an excitation input via feedback routine, as illustrated in Fig. 1, often leading to serious rotor vibration. In Fig. 1, the measured signal contains not only the target runout but also the vibration response caused by the runout through the overall controller of the AMB system. Thus the AMB systems used as high precision spindles require development of accurate scheme for detecting and compensating runouts[3]. Among others, Bently Nevada Corporation[2] developed a runout compensation technique for machine monitoring and diagnosis, which memorizes a slaw-roll wave form and subtracts it from the measured rotor vibration signals contaminated by the runout of probe area; Mitsui[4] investigated a measuring method of spindle rotation accuracy for precision machining based on three points method; Bifano and Dow[5] used a piezoelectric actuator to push a precision spindle against the bearing housing by measuring the master ball motion; Hara and Echigo[3] measured the runout of an ultra precision spindle supported by air bearings, using the three points method and compensated it by using AMBs.

In the previous runout compensation methods developed so far, runout identification process normally requires special arrangement for extra sensors such as a master ball or the three points method, which the rotor is not in service. But

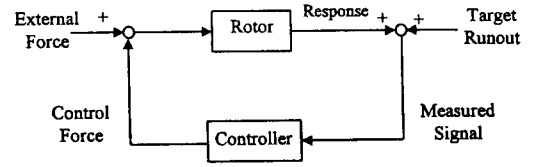

(a) Schematics of signal flow

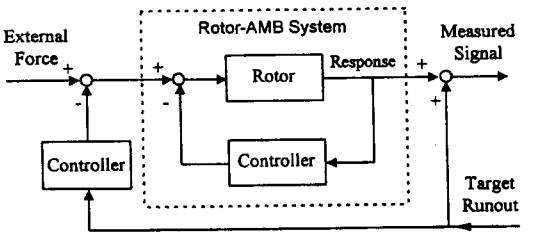

(b) Equivalent block diagram

Fig. 1 Effect of target runout in AMB system.

* 삼성종합기술원

** 한국과학기술원 기계공학과

those elaborate methods can fail in accurate identification of in-situ runout, when the operational condition of interest is far different from that associated with the runout identification process, including the sensors, the sensor locations and the operating speed.

In this study, an in-situ runout identification scheme for AMB spindle system by using extended influence coefficient method[6] is presented and the effect of sensing target runout on the spindle response is studied. The runout identification and compensation scheme is essentially the same as the open loop controller for suppressing unbalance response[7,8], except consideration of higher harmonic components as well as the fundamental harmonic component synchronous to the rotation. Advantages of the proposed scheme are that runout is identified and compensated under a given operating condition, and it does not require any extra device for measurement and compensation of runout.

To verify the effectiveness of the proposed scheme, experiments are performed with the laboratory AMB system, while the system is controlled by DSP-based digital controller under multi-tasking operating condition with a host-PC.

Equation of Motion with Runout

Consider the control loop for active magnetic bearing system with runout and unbalance as shown in Fig. 2: $\boldsymbol{D}_o(s)$, the dynamic stiffness matrix, accounts for the inertia and gyroscopic moments of rotor and the uncontrolled magnetic bearing stiffness; $\boldsymbol{G}_c(s)$ represents the overall transfer function matrix associated with digital control system; $\boldsymbol{K}_s$ is the sensor gain matrix; and $\boldsymbol{G}_f(s)$ represents the electro-magnetic actuators which consist of power amplifiers and electromagnets. The equation of motion for the controlled AMB system can be written, in Laplace domain, as

$$\boldsymbol{D}_o(s)\boldsymbol{Q}(s) = \boldsymbol{F}_u(s) - \boldsymbol{G}_f(s)\boldsymbol{G}_c(s)\boldsymbol{V}_e(s)$$

$$\boldsymbol{V}_e(s) = \boldsymbol{K}_s\{\boldsymbol{Q}(s) + \boldsymbol{R}(s)\} - \boldsymbol{V}_{rc}(s) \qquad (1.a)$$

or

$$\boldsymbol{D}_{cl}(s)\boldsymbol{Q}(s) = -\boldsymbol{G}_f(s)\boldsymbol{G}_c(s)\{\boldsymbol{K}_s\boldsymbol{R}(s) - \boldsymbol{V}_{rc}(s)\} + \boldsymbol{F}_u(s) \qquad (1.b)$$

where

$$\boldsymbol{D}_{cl}(s) = \boldsymbol{D}_o(s) + \boldsymbol{G}_f(s)\boldsymbol{G}_c(s)\boldsymbol{K}_s$$

Here $\boldsymbol{Q}$ is the displacement vector, $\boldsymbol{R}$ is the target runout vector, $\boldsymbol{F}_u$ is the unbalance force vector, $\boldsymbol{V}_e$ is the controller input vector, $\boldsymbol{V}_{rc}$ is the runout compensation signal vector; and $\boldsymbol{D}_{cl}(s)$ is the dynamic matrix of the controlled AMB system. Introducing the relations

$$\boldsymbol{K}_s\boldsymbol{R}_c(s) \equiv \boldsymbol{V}_{rc}(s)$$

$$\boldsymbol{K}_s\boldsymbol{Q}_e(s) \equiv \boldsymbol{V}_e(s)$$

$$\boldsymbol{Q}_e(s) + \boldsymbol{R}_c(s) = \boldsymbol{Q}(s) + \boldsymbol{R}(s)$$

we can rearrange Eq.(1) as

$$\boldsymbol{D}_{cl}(s)\boldsymbol{Q}(s) = -\boldsymbol{G}_f(s)\boldsymbol{G}_c(s)\boldsymbol{K}_s\{\boldsymbol{R}(s) - \boldsymbol{R}_c(s)\} + \boldsymbol{F}_u(s) \qquad (2)$$

It implies that the actual rotor motion $\boldsymbol{Q}$ is affected by runout through the controller dynamics, $\boldsymbol{G}_f(s)\boldsymbol{G}_c(s)\boldsymbol{K}_s$, and the controlled AMB system dynamics, $\boldsymbol{D}_{cl}(s)$. Note here that, once the runout $\boldsymbol{R}$ is identified, the braced term in the right hand side of Eq. (2) can be easily eliminated by letting $\boldsymbol{R}_c(s)=\boldsymbol{R}(s)$ or setting the compensation signal as $\boldsymbol{V}_{rc}(s)=\boldsymbol{K}_s\boldsymbol{R}(s)$. Since $\boldsymbol{Q}$ is not directly measurable, we can rewrite Eq.(2) as

$$\boldsymbol{D}_{cl}(s)\boldsymbol{Q}_e(s) = \boldsymbol{D}_o(s)\{\boldsymbol{R}(s) - \boldsymbol{R}_c(s)\} + \boldsymbol{F}_u(s) \qquad (3)$$

where $\boldsymbol{Q}_e(s)$ is the measurable quantity. Letting $s=j\omega$ and substituting $\boldsymbol{F}_u(j\Omega)=\Omega^2\boldsymbol{U}$ in Eq.(3), we obtain the expression in the frequency domain as

$$\boldsymbol{Q}_e(j\omega) = \boldsymbol{H}_r(j\omega)\{\boldsymbol{R}(j\omega) - \boldsymbol{R}_c(j\omega)\} + \boldsymbol{H}_u(j\omega)\boldsymbol{U} \qquad (4)$$

where

$$\boldsymbol{H}_r(j\omega) = \boldsymbol{D}_{cl}(j\omega)^{-1}\boldsymbol{D}_o(j\omega)$$

$$\boldsymbol{H}_u(j\omega) = \begin{cases} \boldsymbol{D}_{cl}(j\omega)^{-1}\Omega^2 & for\ \omega = \pm\Omega \\ \boldsymbol{0} & otherwise \end{cases}$$

Here Ω is the rotational speed of the rotor, $\boldsymbol{U}$ is the unbalance vector, $\boldsymbol{H}_r(j\omega)$ and $\boldsymbol{H}_u(j\omega)$ are the frequency response matrices between the measured response and the runout and mass unbalance, respectively.

Runout Identification

Runout generates a periodic signal with the period corresponding to each rotor revolution and thus it can be represented in the form of complex Fourier series expansion as

$$r_\theta(\theta) = r_\theta(\theta + 2\pi) = \sum_{k=-\infty}^{\infty} R_{\theta k} e^{jk\theta} \qquad (5)$$

where the Fourier coefficients $R_{\theta k}$ are determined by

$$R_{\theta k} = \frac{1}{2\pi}\int_0^{2\pi} r_\theta(\theta) e^{-jk\theta} d\theta, \quad k = 0, \pm1, \pm2, \ldots$$

Here θ is the shaft rotational angle with respect to the reference axis, y. In magnetic bearing, two identical y- and z-directional proximity sensors are located with right angle. Thus the two measured runout signals $r_y(t)$ and $r_z(t)$ are identical except the time delay with the sensor locations, i.e.

$$r_y(t) = r_\theta(\Omega t) = \sum_{k=-\infty}^{\infty} R_{\theta k} e^{jk\Omega t} \qquad (6)$$

$$r_z(t) = r_\theta(\Omega t - \pi/2) = \sum_{k=-\infty}^{\infty} R_{\theta k} e^{-jk\pi/2} e^{jk\Omega t}$$

Then we can define the complex runout signal as

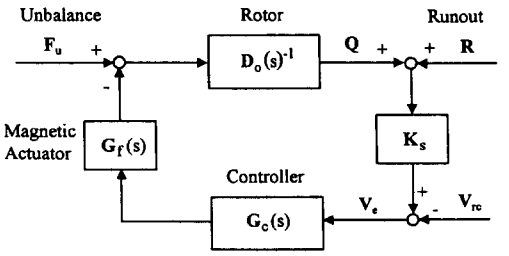

Fig. 2 Block diagram of AMB system with runout and unbalance

$$r(t) = r_y(t) + jr_z(t) = \sum_{k=-\infty}^{\infty} R_k e^{jk\Omega t} \qquad (7.a)$$

where the complex Fourier coefficients R_k are determined by

$$R_k = \frac{\Omega}{2\pi}\int_0^{2\pi/\Omega} r(t)e^{-jk\Omega t}dt, \qquad k = 0,\pm1,\pm2,... \qquad (7.b)$$

Substituting Eq.(6) into Eq.(7.a), we can rewrite Eq.(7.b) as

$$R_k = \left(1 + je^{-jk\pi/2}\right)R_{0k} \qquad (8)$$

Here, the plot of R_k against k will be referred to as the directional spectrum of the complex runout $r(t)$.[9,10]

In a typical AMB system with two radial type magnetic bearings and two measuring planes, as shown in Fig. 3, the measured harmonic response at each sensing plane due to runout becomes, from Eq.(4),

$$Q_e(\omega_k) = \begin{cases} H_r(j\omega_k)R(\omega_k) + H_u(j\omega_k)U & for\ \omega_k = \pm1\Omega \\ H_r(j\omega_k)R(\omega_k) & for\ \omega_k = \pm2\Omega,... \end{cases} \qquad (9)$$

where

$$Q_e(\omega_k) = \begin{Bmatrix} Q_{e1k} \\ Q_{e2k} \end{Bmatrix}, \quad R(\omega_k) = \begin{Bmatrix} R_{1k} \\ R_{2k} \end{Bmatrix}$$

Here Q_{eik} and R_{ik}, i=1,2, ... are the k-th complex Fourier coefficients of the measured signals and the runouts taken from the i-th sensing plane, respectively. Note that the $\pm1\Omega$ component of response is dominantly caused by both runout and unbalance: the response due to runout remains unchanged irrespective of the rotational speed Ω, where as the unbalance response increases rapidly in proportion to Ω^2. Thus, in order to minimize the unbalance response so that the $\pm1\Omega$ component of runout can be extracted from the measured response with fair accuracy, either the mass imbalance of the rotor should be kept small through precision balancing of the AMB system of interest or the rotational speed should be kept as low as possible. On the other hand, higher harmonic components(2Ω, 3Ω,...) of runout can be identified from the rotor response at any rotational speed, since such components are not affected by the unbalance as indicated in Eq.(9). For identification of the runout using Eq.(9), we need to first estimate the runout frequency response matrices $H_r(j\omega)$ evaluated at $\omega=\omega_k=k\Omega$, k=1,2,···. For this purpose, two trial runout signals, R_{t1} and R_{t2}, are applied to each AMB at a given speed. From the three test runs at the same speed, one original and two trial runs, we can construct the following relations :

- from the original test run;

$$Q_{e0}(\omega_k) = H_{r1}(j\omega_k)R_{1k} + H_{r2}(j\omega_k)R_{2k} \qquad (10.a)$$

- for the trial runout R_{t1};

$$\begin{aligned} Q_{e1}(\omega_k) &= H_{r1}(j\omega_k)\left[R_{1k} + R_{t1k}\right] + H_{r2}(j\omega_k)R_{2k} \\ &= Q_{e0}(\omega_k) + H_{r1}(j\omega_k)R_{t1k} \end{aligned} \qquad (10.b)$$

- for the trial runout R_{t2};

$$\begin{aligned} Q_{e2}(\omega_k) &= H_{r1}(j\omega_k)R_{1k} + H_{r2}(j\omega_k)\left[R_{2k} + R_{t2k}\right] \\ &= Q_{e0}(\omega_k) + H_{r2}(j\omega_k)R_{t2k} \end{aligned} \qquad (10.c)$$

where the 2×2 influence coefficient matrix is defined as

$$H_r(j\omega_k) = \left[H_{r1}(j\omega_k) | H_{r2}(j\omega_k)\right] \quad \omega_k = k\Omega,\ k = \pm1,\pm2,...$$

Here Q_{e0}, Q_{e1} and Q_{e2} are the original response vector and the response vectors due to trial runout R_{t1} and R_{t2}, respectively. The influence coefficients are obtained from Eq. (10) as

$$\begin{aligned} H_{r1}(j\omega_k) &= \left\{Q_{e1}(\omega_k) - Q_{e0}(\omega_k)\right\} / R_{t1k} \\ H_{r2}(j\omega_k) &= \left\{Q_{e2}(\omega_k) - Q_{e0}(\omega_k)\right\} / R_{t2k} \end{aligned} \qquad (11)$$

where, $\omega_k = k\Omega,\ k = \pm1, \pm2, ...$

Substituting Eq.(11) into Eq.(10.a), we can obtain the estimate for target runout as

$$R(\omega_k) = \begin{Bmatrix} R_{1k} \\ R_{2k} \end{Bmatrix} = \left[H_{r1}(j\omega_k) | H_{r2}(j\omega_k)\right]^{-1} Q_{e0}(\omega_k) \qquad (12)$$

where, $\omega_k = k\Omega,\ k = \pm1, \pm2, ...$

Finally the runout signals at each AMB can be generated from Eqs. (12) and (7). Note that the runout identification scheme explained above is essentially the same as the well known two plane rigid rotor balancing[9], except the consideration of higher harmonic components as well as the synchronous component.

Experimental Result

Experimental Setup

Figure 4 shows the overall block diagram of the AMB system, which consists of a rotor, two radial magnetic bearings, four eddy current type proximity probes, a digital controller using digital signal processor(DSP) with A/D and D/A converters, four PWM power amplifiers, a host PC and a driving motor. The rotor is composed of two magnet journals, two sensing journals and a motor armature located between two AMBs. The rotor rotational angle is measured by an incremental encoder(360 pulse/rev) and fed to the DSP board. The host PC is linked to DSP via dual-port memory in the DSP board, providing a multi-tasking operating condition. The PC downloads the instruction codes, control gains and runout data to DSP board, monitors the operating condition of the AMB system, and executes the runout identification procedure using transferred response signals. While, in the digital control system with DSP, 4-input/4-output control action is performed with the overall control period of 50μsec (20kHz) and the open loop runout

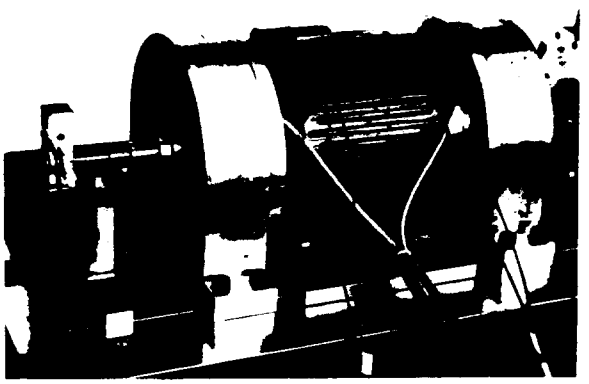

Fig. 3 Perspective view of AMB system

compensation is proceeded using the rotation synchronous encoder signal. For the tested AMB system shown in Fig.3, the rotor mass is 8.34kg, the bearing span length is 277 mm, and the diameter of the magnet and sensing journal is 89 mm.

Runout Estimation Result

In order to estimate the influence coefficients defined in Eqs. (10) and (11), trial runout signals with 30 harmonic components were input to the DSP memory and the resulting responses were captured by the host PC. During the test, the control gains and the rotational speed remained unchanged. Since the sampled data are essentially periodic with the period of one revolution, rotation angle based discrete complex Fourier transformation of the measured signal was performed, only requiring the rectangular windowing to avoid spectral leakage. Then the complex Fourier coefficients of the runout calculated from Eq. (12) were substituted into Eq.(7), in order to generate the estimated runout signals in the time do main. Finally the runout signals were loaded to the DSP memory to measure the runout compensated responses.

Figures 5 and 6 show the measured responses at each AMB and the corresponding directional spectra when the AMB system was run at 2000rpm without runout compensation. Here the y- and z-directional responses are very similar only with the 90 degrees phase difference, which is owing to the isotropic control of AMB system[11]. Note that the response at AMB-1 is dominated by the second harmonic component and that the response at AMB-2 has the magnitude less than 10μm and the wide frequency band. Figures 7 and 8 are the estimated runout signals at each AMB and the corresponding directional spectra at 2000rpm. The estimated runout at AMB-1, as shown in Figs. 7(a) and 8(a), is mainly composed of the first and second harmonic components. It indicates that the presence of a short duration spike in the responses shown in Fig.5(a) is due to the runout at AMB-1. The estimated runout at AMB-2 shown in Figs. 7(b) and 8(b) is also dominated by the first and second harmonics, but their amplitudes are far smaller than those of AMB-1. The directional spectra of the estimated runout, shown in Fig.8, well agree with the relation in Eq.(8) and this shows the indirect verification of the estimated runout.

Figure 9 shows the actual vibration response of the AMB rotor at 2000rpm due to the target runouts, which is obtained using the relation $\boldsymbol{Q}=\boldsymbol{Q}_e(\theta)-\boldsymbol{R}(\theta)$, i.e., by subtracting the estimated runout signals shown in Fig.7 from the measured responses shown in Fig.5. Comparison of Figs. 5 and 9 indicates that the runout signal tends to destabilize the AMB system at 2000 rpm. In fact, it was found that the second harmonic component of runout is fed back through the control loop of the AMB and it excites the fundamental resonant mode at 74 Hz of the AMB system.

Figure 10 shows the whirl responses of the AMB system with runout compensation. It clearly evidences that the target runouts were effectively identified and removed, resulting in that the runout compensated signals remained within the sensor resolution of 0.5μm. Figure 11 compares the maximum whirl responses at each AMB with and without runout compensation as the rotational speed is varied. Here the runout is identified at each operating speed. Once the runout is identified, at a speed, it can be used as the

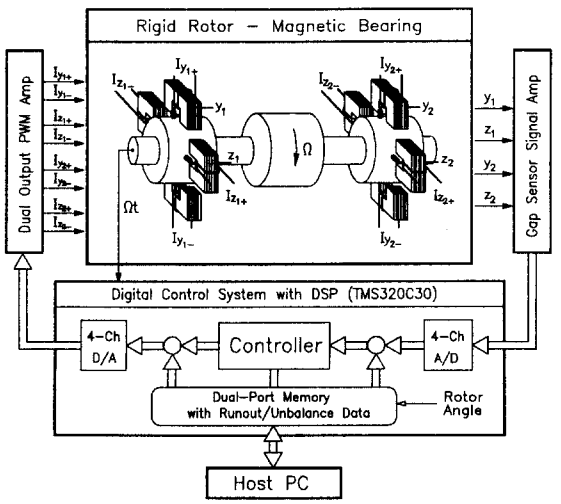

Fig.4 Schematics of rigid rotor-AMB system with digital controller

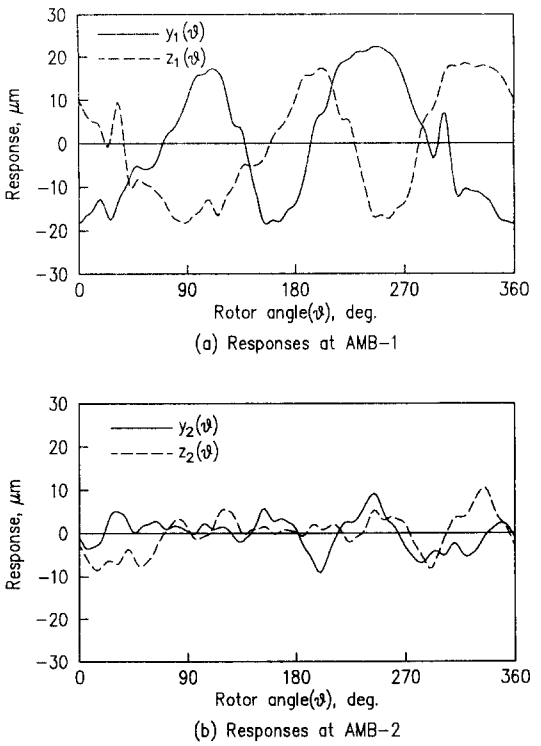

Fig.5 Measured responses of AMB system at 2000rpm without runout compensation

compensation signal for other speeds. However, since the runout signal is likely to be influenced by the operating speed due to the sensing system dynamics, it is more desirable to estimate runout at each operating condition for precision operation. The proposed runout estimation scheme is very simple to use and it takes less than one minute, including data acquisition time.

Conclusion

The effect of sensing target runout on the rotor response is formulated for active magnetic bearing system and an efficient, yet easy to use in-situ runout identification scheme by extended influence coefficient method is proposed. The experimental results show that the proposed scheme works excellently with the well balanced AMB system over the wide operating speed range.

References

1. Brunet, M., 1988, "Practical Applications of the Magnetic Bearings to the Industrial World," 1st International Symposium on Magnetic Bearings, Zurich, pp. 225-244.
2. Bently Nevada Corporation, 1979, "Vector Nulling versus Runout Compensation," Application Note, No. L0196.
3. Hara, S., and Echigo, K., 1992, "A Trial Product of Ultra Precision Spindle," 3rd International Symposium on Magnetic Bearings, Alexandria, pp. 421-428.
4. Mitsui, K., 1992, "Development of New Measuring Method for Spindle Rotating Accuracy by Three Points Method," Proceedings of 23rd International MTDR Conference, pp.195-121.
5. Bifano, T. G., and Dow, T. A., 1985, "Real Time Control of Spindle Runout," Optical Engineering, Vol.34, No. 5, pp. 888-892.
6. Kim, C. S., 1995, *Dynamic Analysis and Isotropic Optimal Control of Active Magnetic Bearing System*, Ph. D Dissertation Paper, KAIST, pp.87-116.
7. Higuchi, T., Otsuka, M., Mizuno, T., and Ide, T., 1990, "Application of Periodic Learning Control with Inverse Transfer Function Compensation in Totally Active Magnetic Bearings," 2nd International Symposium on Magnetic Bearings, Tokyo, pp. 257-264.
8. Knospe, C. R., Hope, R. W., Fedigan, S. J., and Williams, R. D., 1993, "Adaptive On-Line Rotor Balancing Using Digital Control," Proceedings of MAG'93 Magnetic Bearings, Magnetic Drives, and Dry Gas Seals Conference, Alexandria, pp. 153-164.
9. Lee, C. W., 1993, *Vibration Analysis of Rotors*, Kluwer Academic Publishers, pp. 215-221.
10. Lee, C. W. and Joh, C.Y., 1994, "Use of Directional Spectra for Diagnosis of Asymmetry / Anisotropy in Rotor Systems," Proceedings of the Fourth International Conference on Rotor Dynamics, Chicago, pp.97-101.
11. Kim, C.S. and Lee, C. W., 1994, "Isotropic Optimal Control of Active Magnetic Bearing System," 4th International Symposium on Magnetic Bearings, Zurich.

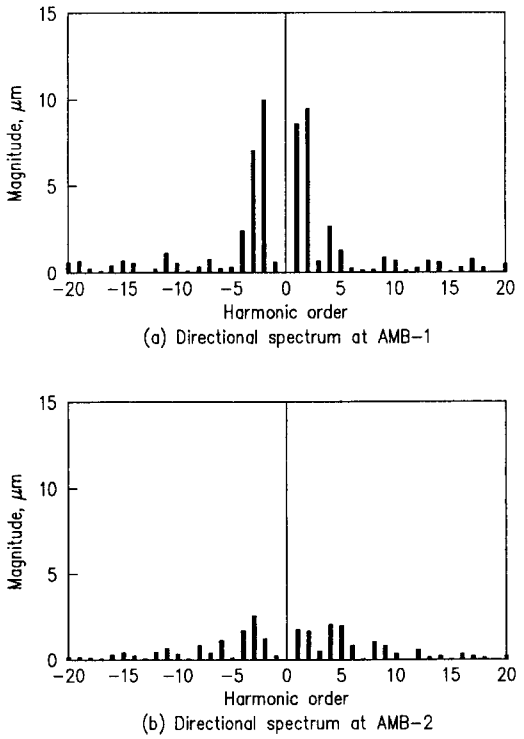

Fig.6 Directional spectra of measured responses at 2000rpm without runout compensation

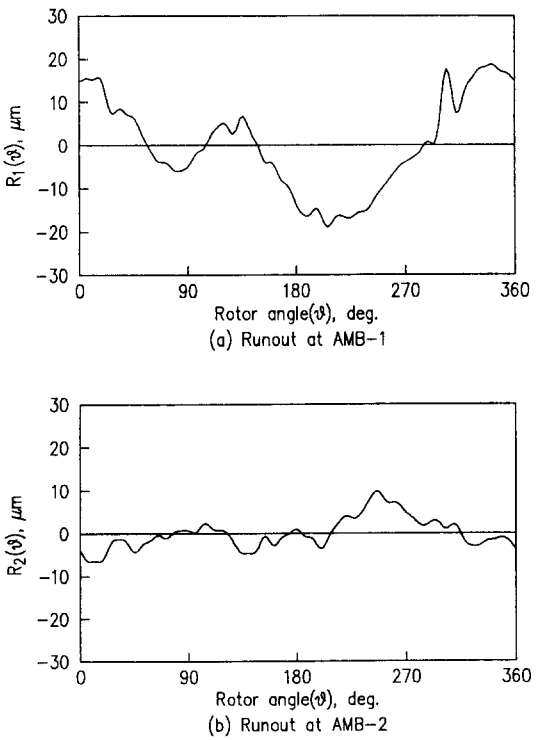

Fig.7 Estimated target runouts of AMB at 2000rpm

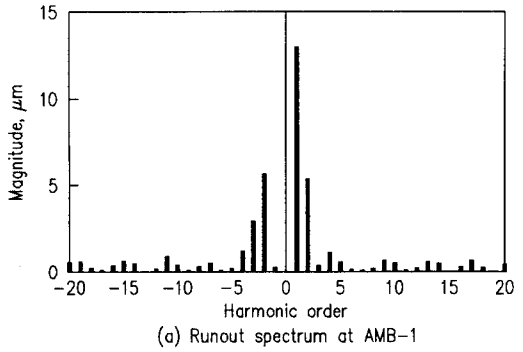

(a) Runout spectrum at AMB-1

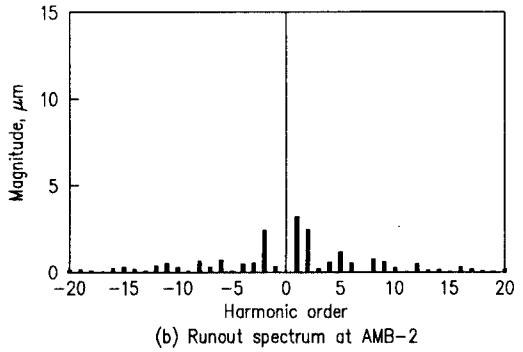

(b) Runout spectrum at AMB-2

Fig.8 Directional spectra of estimated runout of AMB at 2000rpm

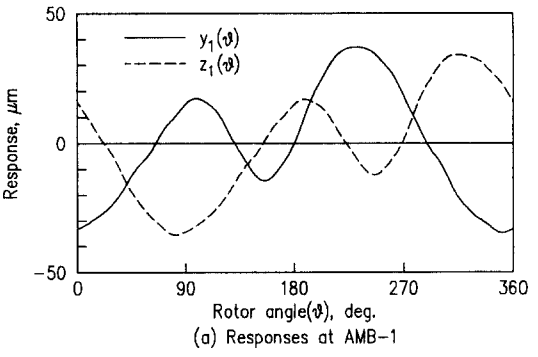

(a) Responses at AMB-1

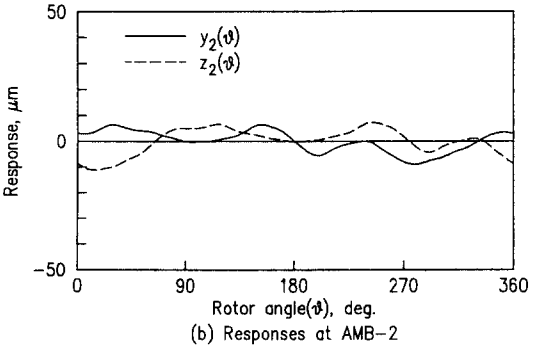

(b) Responses at AMB-2

Fig.9 Actual responses of AMB system at 2000rpm due to target runouts

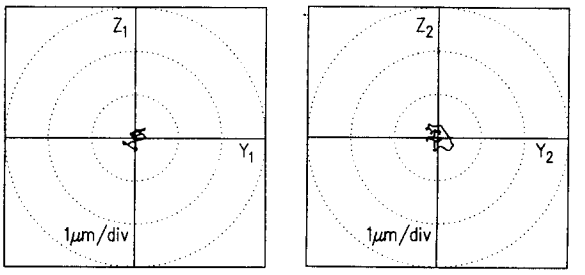

(a) Whirl at AMB-1 (b) Whirl at AMB-2

Fig.10 Whirl of AMB with runout compensation at 2000rpm

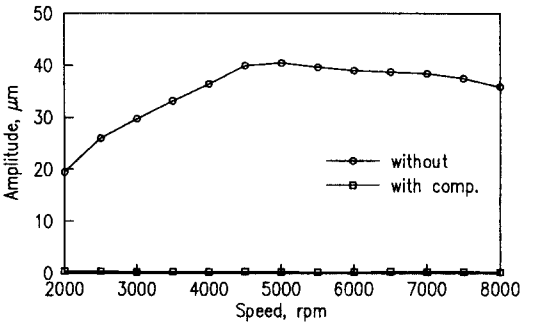

(a) Response amplitude at AMB-1

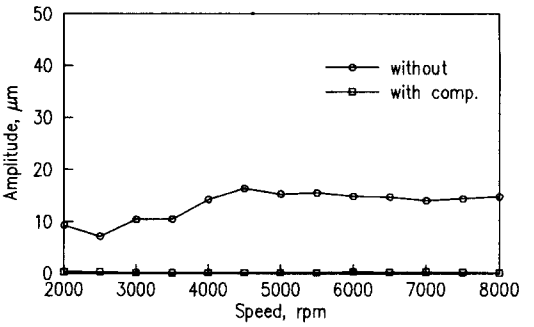

(b) Response amplitude of AMB-2

Fig.11 Maximum amplitude of AMB with and without runout compensation